J|A|C|S
ARTICLES
Published on Web 03/09/2002

Nearly Monodisperse and Shape-Controlled CdSe Nanocrystals via Alternative Routes: Nucleation and Growth

Z. Adam Peng and Xiaogang Peng*

Contribution from the Department of Chemistry and Biochemistry, University of Arkansas, Fayetteville, Arkansas 72701

Received October 17, 2001

Abstract: The nucleation and growth of colloidal CdSe nanocrystals with a variety of elongated shapes were explored in detail. The critical size nuclei for the system were magic sized nanoclusters, which possessed a sharp and dominated absorption peak at 349 nm. The formation of the unique magic sized nuclei in a broad monomer concentration range was not expected by the classic nucleation theory. We propose that this was a result of the extremely high chemical potential environment, that is, very high monomer concentrations in the solution, required for the growth of those elongated nanocrystals. The shape, size, and size/shape distributions of the resulting nanocrystals were all determined by two related factors, the magic sized nuclei and the concentration of the remaining monomers after the initial nucleation stage. Without any size sorting, nearly monodisperse CdSe quantum structures with different shapes were reproducibly synthesized by using the alternative cadmium precursors, cadmium-phosphonic acid complexes. A reasonably large excess of the cadmium precursor, which is less reactive than the Se precursor, was found beneficial for the system to reach the desired balance between nucleation and growth. The shape evolution and growth kinetics of these elongated nanocrystals were consistent with the diffusion-controlled model proposed previously. The branched nanocrystals had to grow at very high monomer concentrations because the multiple growth centers at the end of each branch must be fed with a very high diffusion flux to keep all branches in the 1D-growth mode. The rice-shaped nanocrystals were found as special products of the 3D-growth stage. The growth of the nanocrystals in the 1D-growth stage was proven to be not unidirectional after the length of the nanocrystals reached a certain threshold. Experimental results indicate that coordinating solvents and two ligands with distinguishable coordinating abilities are both not intrinsic requirements for the growth of elongated CdSe nanocrystals.

Introduction

Colloidal nanocrystals have attracted much attention for their distinguishable role in fundamental studies and technical applications,[1,2] mainly due to their size-dependent properties and flexible processing chemistry. In a restricted sense, recent reports indicate that the size dependence mentioned here should refer to the size along all three dimensions, that is, the volume and the shape. Rod- or wire-shaped semiconductor nanocrystals possess clearly different optical properties in comparison to their dot-shaped analogues.[3−5] The magnetic dipole moment may take the long axis of magnetic nanocrystals as the easy axis, which is desirable for magnetic information storage.[6] The catalytic properties of various types of colloidal nanocrystals have also been suspected to be dependent on their shape.[7] In addition to their unique properties, the anisotropic shapes of nanocrystals can be exploited as an alignment handler for the long- and short-range assembly of these nanostructures.[5,8] The shape evolution of colloidal nanocrystals can also be employed as a sensitive probe for studying crystallization processes.[9] Such studies have benefited and will continue to benefit the development of synthetic chemistry for colloidal nanocrystals with a desired shape control.

Studies of the shape control of colloidal nanocrystals may further provide some insight for understanding this important phenomenon in general. By and large, shape control in crystallization is unknown.[10] The most referred classic model for shape control is the Wulff facets argument, or Gibbs−Curie−Wulff theorem, which suggests that the shape of a crystal is determined by the relative specific surface energy of each face or facet of the crystal.[10] However, our recent results unambiguously reveal that this pure thermodynamic argument is unlikely useful for the understanding of any shape evolution, which occurs far away from the thermodynamic equilibrium and must be overdriven

* To whom correspondence should be addressed. Phone: 501-575-4612. Fax: 501-575-4049. E-mail: xpeng@uark.edu.

(1) Heath, J. R., Ed. *Acc. Chem. Res.* **1999**, *Special Issue for Nanostructures*, review articles relevant to colloidal nanocrystals.
(2) Alivisatos, A. P. *Science* **1996**, *271*, 933−937.
(3) Wang, J.; Gudiksen, M. S.; Duan, X.; Cui, Y.; Lieber, C. M. *Science* **2001**, *293*, 1455.
(4) Hu, J.; Li, L.-s.; Yang, W.; Manna, L.; Wang, L.-w.; Alivisatos, A. P. *Science* **2001**, *292*, 2060.
(5) Peng, X. G.; Manna, L.; Yang, W. D.; Wickham, J.; Scher, E.; Kadavanich, A.; Alivisatos, A. P. *Nature* **2000**, *404*, 59.
(6) Puntes, V. F.; Krishnan, K. M.; Alivisatos, A. P. *Science* **2001**, *291*, 2115.
(7) Ahmadi, T. S.; Wang, Z. L.; Green, T. C.; Henglein, A.; El-Sayed, M. A. *Science* **1996**, *272*, 1924.
(8) Kim, F.; Kwan, S.; Akana, J.; Yang, P. *J. Am. Chem. Soc.* **2001**, *123*, 4360.
(9) Peng, Z. A.; Peng, X. G. *J. Am. Chem. Soc.* **2001**, *123*, 1389.
(10) Mullin, J. W. *Crystallization*, 3rd ed.; Oxford, 1997.

by high monomer concentrations.[9] The other fundamental significance for studying the shape control and shape evolution of colloidal nanocrystals lies on the understanding of nucleation. At present, nucleation is poorly understood, due to a lack of reliable experimental data.[10] The extreme growth conditions required for the elongated shapes of colloidal nanocrystals provide a sensitive test ground for nucleation theories.

In comparison to other nanocrystal systems, the study of the shape evolution of colloidal CdSe nanocrystals is advantageous. First, the size/shape-dependent optical properties of semiconductor nanocrystals can be used as convenient probes to study the growth and shape evolution of these nanocrystals. Second, the semiconductor nanocrystal systems, especially CdSe nanocrystals, are more or less the best studied colloidal nanocrystal systems in terms of size and shape control.[5,9,11,12] The knowledge learned from the chosen model systems should be extendable to other colloidal nanocrystal systems. Historically, the growth mechanisms of wire- or whiskers-shaped microcrystals in gas phase through the vapor−liquid−solid (VLS) growth mode were established in the middle of last century.[13] Today, such understanding has resulted in the growth of a large variety of nanorods and nanowires using VLS[3,13−15] and its alternatives.[16,17]

The synthesis of rod-shaped CdSe colloidal nanocrystals with their short axis smaller than the quantum-confined size regime (CdSe quantum rods) was reported in year 2000[5] through the traditional organometallic approach using dimethyl cadmium, an extremely dangerous organometallic compound, as the cadmium precursor in a coordinating solvent composed of trioctylphosphine oxide (TOPO) and hexylphosphonic acid (HPA). We recently reported that similar results can be obtained using those safe, inexpensive, and minimum toxicity cadmium precursors, such as cadmium oxide.[18] CdTe quantum rods were also synthesized with these alternative precursors.[18] In addition to this development, CdS nanorods and related nanostructures were also synthesized in pure hexyldecylamine using a single precursor containing both cadmium and sulfur.[19]

The chemical potential of elongated nanocrystals should be generally higher than that of a dot-shaped nanocrystal if the unit cell of the corresponding crystal structure is not highly distorted along a certain axis. As a result, the growth of such anisotropic structures should require a relatively high chemical potential environment in the solution, that is, a relatively high monomer concentration.[5,9,11,18] This condition provides the external environment for the formation of elongated[5,9,11,18] or other anisotropic shapes.[11,19] For CdSe nanocrystals, their wurtzite structure possesses a unique *c*-axis, which provides an intrinsic broken symmetry along this axis.[5,9,11,18] Experimental results indicate that, for diffusion-controlled growth, the distribution of incoming diffusion flux toward each nanocrystal depends strongly on the monomer concentration in the bulk solution.[9] At high monomer concentrations, the incoming monomers diffused into the diffusion sphere are mainly consumed by the facets perpendicular to the *c*-axis of the CdSe nanocrystals, which results in a "one-dimensional growth" stage, or 1D-growth stage. With intermediate monomer concentrations, the incoming monomers are shared by all the facets, and a "three-dimensional growth" stage (3D-growth stage) exists. If the chemical potential of the monomers in the bulk solution is comparable to the overall chemical potential of the entire crystal, there is no net diffusion flux between the bulk solution and the diffusion sphere. The monomers on the surface of nanocrystals adjust their positions to minimize the total surface energy of a given crystal, which means a rod-shaped crystal will eventually become a dot-shaped one. This stage is called "one-dimension to two-dimension intraparticle ripening", or simply 1D/2D-ripening. A further lower monomer concentration will eventually intrigue Ostwald ripening occurring in an interparticle manner.

The results shown below will emphasize several critical issues which need to be addressed for further understanding of the diffusion-controlled mechanisms as well as designing a better synthetic strategy. The first issue is the nucleation process for the formation of rod-shaped and other elongated nanostructures, which is the first and also the key step for the growth of nanocrystals with anisotropic shapes. The second question is the function of the coordinating solvent and the two ligands with distinguishable coordinating abilities to the surface atoms of nanocrystals. Because the formation of CdSe nanocrystals has been performed in a coordinating solvent composed of TOPO and phosphonic acids,[5,9,11,18] several research groups suggested that coordinating solvent, two ligands with distinguishable binding abilities, and a fixed ratio range of the two ligands are prerequisites for the formation of rod-shaped nanocrystals. The third issue to be addressed is the growing direction in the 1D-growth stage. For wurtzite CdSe, the unique *c*-axis has always been observed as the long axis of those elongated nanostructures.[6,11,20,21] Manna et al. suggested that the growth is only along the (001) direction or the selenium terminated facet of an equilibrium crystal on the basis of the appearance of some pointed structures carefully resolved under a high-resolution transmission electron microscope (TEM).[11] The final major issue is the compatibility of the development of the shape-controlled synthesis and the further implementation of green chemistry principles into the synthetic chemistry. Up to the present, the control of the shape and size/shape distribution of semiconductor nanorods and quantum rods is not well developed. The other elongated shapes to be described below were either never before observed or lack a reliable controllable synthetic scheme to make them. Our intention is to solve these synthetic challenges through the recently developed alternative routes[18,22−24] with the help of the further understanding of the growth mechanisms.

Experimental Section

Chemicals. CdO (99.99%), tributylphosphine (TBP), trioctylphosphine (TOP), 99% TOPO, technical grade 1-octadecene (ODE), and selenium powder were purchased from Aldrich. Methanol, toluene,

(11) Manna, L.; Scher, E. C.; Alivisatos, A. P. *J. Am. Chem. Soc.* **2000**, *122*, 12700.
(12) Peng, X. G.; Wickham, J.; Alivisatos, A. P. *J. Am. Chem. Soc.* **1998**, *120*, 5343.
(13) Lieber, C. M. *Solid State Commun.* **1998**, *107*, 607.
(14) Wong, E. W.; Maynor, B. W.; Burns, L. D.; Lieber, C. M. *Chem. Mater.* **1996**, *8*, 2041.
(15) Morales, A. M.; Lieber, C. M. *Science* **1998**, *279*, 208.
(16) Holmes, J. D.; Johnston, K. P.; Doty, R. C.; Korgel, B. A. *Science* **2000**, *287*, 1471.
(17) Trentler, T. J.; Hickman, K. M.; Goel, S. C.; Viano, A. M.; Gibbons, P. C.; Buhro, W. E. *Science* **1995**, *270*, 1791.
(18) Peng, Z. A.; Peng, X. *J. Am. Chem. Soc.* **2001**, *123*, 183−184.
(19) Jun, Y.-w.; Lee, S.-M.; Kang, N.-J.; Cheon, J. *J. Am. Chem. Soc.* **2001**, *123*, 5150.
(20) Malik, M. A.; Revaprasadu, N.; O'Brien, P. *Chem. Mater.* **2001**, *13*, 913.
(21) Soulantica, K.; Maisonnat, A.; Fromen, M. C.; Casanove, M. J.; Lecante, P.; Chaudret, B. *Angew. Chem. Int. Ed.* **2001**, *40*, 2984.
(22) Qu, L.; Peng, X. *J. Am. Chem. Soc.*, in press.
(23) Qu, L.; Peng, Z. A.; Peng, X. *Nano Lett.* **2001**, *1*, 333.
(24) Peng, X. *Chem.-Eur. J.*, in press.

hexanes, and diethyl ether were purchased from VWR. Tetradecylphosphonic acid (TDPA) and octadecyl phosphonic acid (ODPA) were purchased from Alfa. HPA was synthesized using the method reported previously.[9]

Synthesis of Cadmium-TDPA (Cd-TDPA) and Cadmium-ODPA (Cd-ODPA) Complexes. CdO (0.6420 g, 5 mmol) and TDPA (2.7900 g, 10 mmol) with 2 g of TOPO (or ODPA (3.3447 g, 10 mmol) with 2.2 g of TOPO) were loaded into the reaction flask and then heated under argon flow. The mixture turned optically clear at around 300 °C in TDPA/TOPO solution or 200 °C in ODPA/TOPO solution. After the solution was kept at the dissolving temperatures for 5−10 min, it was allowed to cool to room temperatures under argon flow. A solid product was obtained and was then taken out from the reaction flask. For the quasi-one-pot synthesis, the Cd-TDPA or Cd-ODPA complex after aging for at least 24 h was used directly without further purifications. For the two-pot synthesis, the pure Cd-TDPA or Cd-ODPA complex was isolated by washing the unpurified products with large amounts of methanol repeatedly. Except for those mentioned, Cd-TDPA and Cd-ODPA will always refer to the *unpurified and aged* complexes in this paper.

Detailed Synthetic Procedures. The detailed synthetic procedures for different shaped nanocrystals through a variety of approaches are provided in the Supporting Information.

Recovery and Characterization of the Ligands on the Surface of CdSe Quantum Rods. The ligand-coated CdSe rods dissolved in toluene were precipitated in methanol. The precipitate was isolated by centrifugation, decantation, and washed with methanol three times. The nanocrystals were then redissolved by toluene and then separated from the insoluble part by centrifugation/decantation processes. The toluene solution of the nanocrystals was further treated by methanol to precipitate the CdSe nanocrystals, and the purified nanocrystal precipitate was isolated by centrifugation/decantation and dried under vacuum. The nanocrystal powder was destroyed in a standard HCl/HNO_3 digestion solution for atomic absorption measurements. The organic phase of the digestion solution was extracted by ethyl ether and washed by pure water three times. After evaporation of ethyl ether, the white solid was characterized using H^1 NMR spectra in *d*-chloroform ($CDCl_3$).

Monitoring the Reactions and Characterizing the Resulting Nanocrystals. In the experiments, needle-tip aliquots were taken from the reaction flask at given time intervals and dissolved in about 1 mL of hexanes. UV−vis absorption spectra were recorded with a HP 8453 diode array spectrophotometer for each aliquot. For the TEM imaging, nanocrystals were deposited onto the Formvar-coated copper grids and observed using a JEOL 100 CX TEM. A Philips PW1830 X-ray powder diffractometer was employed to check the crystallinity of the nanocrystals. Statistical evaluations included all the nanocrystals in a chosen area of a TEM micrograph (about 500 ± 50 particles). The volume of a given nanocrystal was approximated as the product of its long axis dimension times the square of its short axis dimension.

Results

Because this work was intended to understand the nucleation and growth processes related to the formation of shape-controlled nanocrystals, no size sorting was performed for all of the samples used for the measurements to be discussed below.

Effects of Cadmium Precursors. Ideally, a system should form a relatively small amount of nuclei in a short period of time, and these formed nuclei will not consume the remaining monomers in a noticeable manner as they grow quickly to a desired elongated shape.[5,9,11,18] Certainly, relatively less reactive precursors would be helpful. In principle, the alternative cadmium precursors are all more stable than dimethyl cadmium, and they should be more suited for the growth of anisotropic nanostructures. We chose cadmium-phosphonic acid complexes as the cadmium precursors, which are less reactive than the other soluble precursors, such as the fatty acid salts. In fact, the cadmium monomers at the growth stage were actually cadmium-phosphonic acid complexes when dimethyl cadmium was used as the cadmium precursor.[9]

We observed that the reactivity of the cadmium phosphonic acid complexes, for example, Cd-TDPA, noticeably depended on its history. In a direct-one-pot approach, Cd-TDPA was formed by heating the mixture of CdO, TDPA, and TOPO to the desired injection temperature, which resulted in an optically clear solution. After the injection of cold selenium solution into this hot solution, the reaction mixture changed from colorless to yellowish in about 2 min. The highest aspect ratio of the resulting rods through this direct-one-pot synthesis (Figure 1 b) is about three. However, if the cadmium solution was cooled to room temperature and aged for a few days (see Experimental Section), the growth reaction of this quasi-one-pot synthesis was significantly slower. The color of the reaction mixture changed from colorless to yellowish at about 4 min after the injection of the cold selenium solution. Although the dimension of the short axis did not change noticeably, the highest average aspect ratio of the resulting nanocrystals of this quasi-one-pot synthesis was about 6.5 (Figure 1). Below, all synthetic reactions were performed using this quasi-one-pot approach. The third approach was the two-pot synthesis (see Supporting Information), in which purified Cd-TDPA was mixed back with TOPO in an identical composition to the other two approaches. The structural features of the resulting products of this two-pot reaction were almost identical to those of the quasi-one-pot approach.

It was observed that the complex formed at high temperatures by dissolving $Cd(CH_3)_2$ in TOPO/HPA mixture was a cadmium complex with both TOPO and HPA as ligands.[9] Such a complex was not stable after cooling to room temperatures and slowly decomposed to a Cd-HPA complex without any TOPO as its ligands. A similar process occurred in the experiments described above. By aging it at room temperatures, the complex formed by dissolving CdO in the hot TOPO/TDPA mixture was converted to the desired Cd-TDPA complex, which is more stable than the one without aging. Consequently, this more stable Cd-TDPA complex slowed the nucleation process and formed less nuclei in the initial stage, and the concentration of the remaining monomers after the nucleation process was always higher than that of the direct-one-pot synthesis (see below for more evidences), which provided the desired balance between the nucleation and growth processes.

Magic Sized Nanoclusters. Magic sized nanoclusters of CdSe are those CdSe clusters with defined molecular structures in the size range between 1 and 2 nm. Typically, they contain no more than one unit cell of the bulk crystal and possess close-shell structures.[25] Because of the close-shell configuration, these nanoclusters are thermodynamically more stable than the clusters which are either a little smaller or a little bigger but without a close-shell structure. Therefore, magic sized nanoclusters appear always at fixed and discrete sizes. Experimentally, magic sized nanoclusters of semiconductors can be detected by the appearance of sharp absorption peaks at persistent and isolated positions.

Two distinguishable persistent absorption peaks were repeatedly observed in the current system, with an absorption peak at

(25) Soloviev, V. N.; Eichhofer, A.; Fenske, D.; Banin, U. *J. Am. Chem. Soc.* **2000**, *122*, 2673.

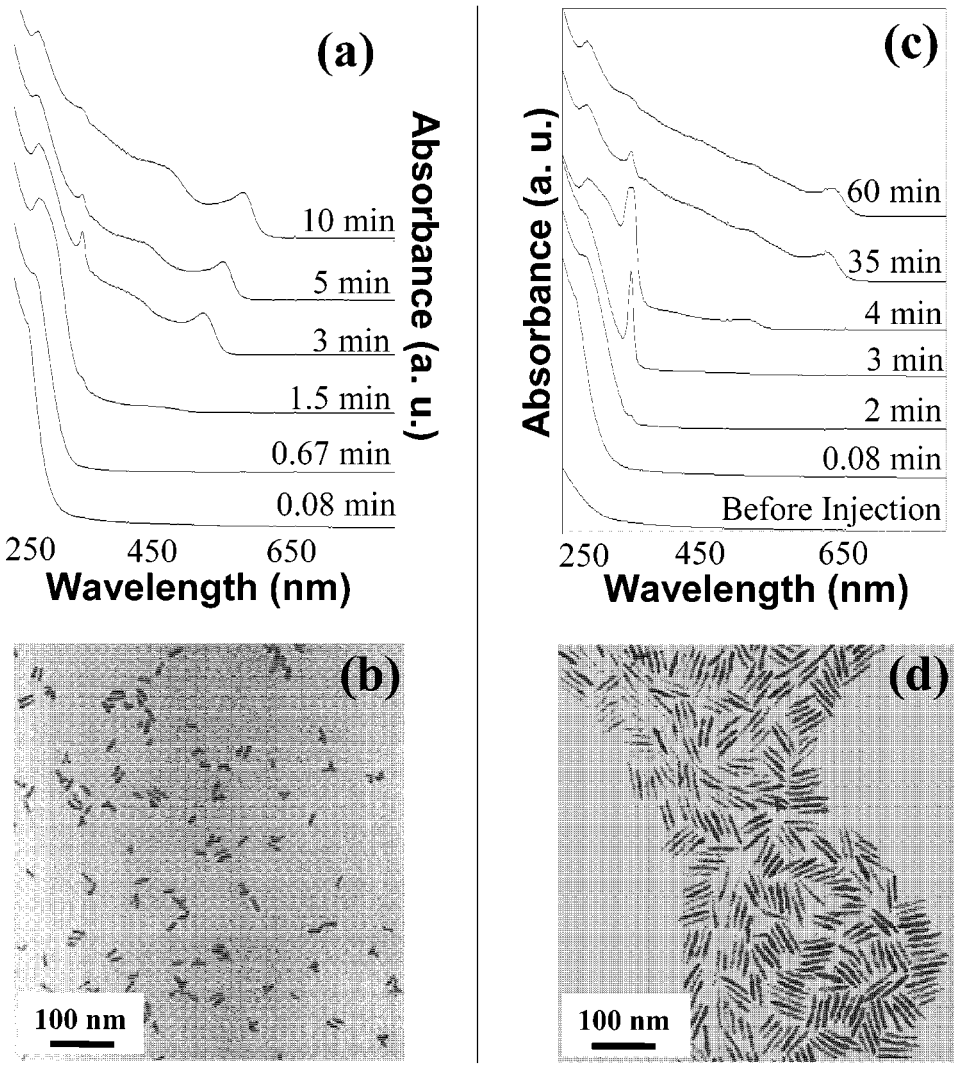

Figure 1. Influence of the history of Cd-TDPA complexes. Left panel: Without aging at room temperature. Right panel: Aged at room temperatures. TEM pictures were taken with the aliquots with the highest average aspect ratio in each reaction.

about 285 nm and at exactly 349 nm, respectively (see Figure 1). The peak at 349 nm is close to that of the CdSe clusters containing 17 Cd atoms (Cd17) reported by Soloviev et al.,[25] suggesting a similar sized magic nanocluster appeared in the current system. However, the peak observed by us is much sharper (see Figure 1, especially the 3 min aliquots on the right panel) than the ones observed by Soloviev et al.,[25] which could be a result of the different nature of the ligands.

The other persistent absorption feature observed at about 285 nm is different from the other at 349 nm. This one is not very sharp and lasts normally for the entire growth course. It is clearly not due to the absorption of the Cd-TDPA complex or Se-TBP because it only appeared around a few seconds after the injection of the selenium solution (see Figure 1c). The related CdSe structure should be something significantly smaller than a cluster with four cadmium atoms observed by Soloviev et al.[25] because of the exceptionally high absorption energy. Likely, it is a CdSe molecule, instead of a magic sized nanocluster.

The rate of the appearance of the magic sized nanoclusters should be a reliable measure of the nucleation rate. Furthermore, since the magic sized nanoclusters should only be stable at relatively high monomer concentrations due to their extremely small sizes, the existence of the nanoclusters can be considered as an indicator of the high monomer concentration in the reaction solution. The peak at 349 nm appeared shortly after the injection and became a shoulder 10 min after the injection for the direct-one-pot synthesis shown in Figure 1, left panel. On the contrast, for the quasi-one-pot synthesis, it was a very sharp and dominated feature at 4 min of the injection and lasted for more than 35 min as a distinguishable peak in the spectrum (Figure 1, right panel). These results suggest two related conclusions. First, the nucleation process of the direct-one-pot synthesis occurred in a faster rate and consumed more monomers in comparison to that in the case of the quasi-one-pot synthesis, and formed more nuclei than that of the quasi-one-pot synthesis. Second, the monomer concentration at a given reaction time for the direct-one-pot synthesis was always lower than that of the quasi-one-pot synthesis, although the initial monomer concentrations for the two cases were identical. Consequently, the relatively high and stable monomer concentrations and the small amount of nuclei in the case of the quasi-one-pot synthesis promoted the formation of the rods with a high aspect ratio (Figure 1).

Minimum Short Axis. The temporal evolution of the absorption spectrum of the CdSe nanostructures showed a stage of the coexistence of the magic sized nanoclusters and some

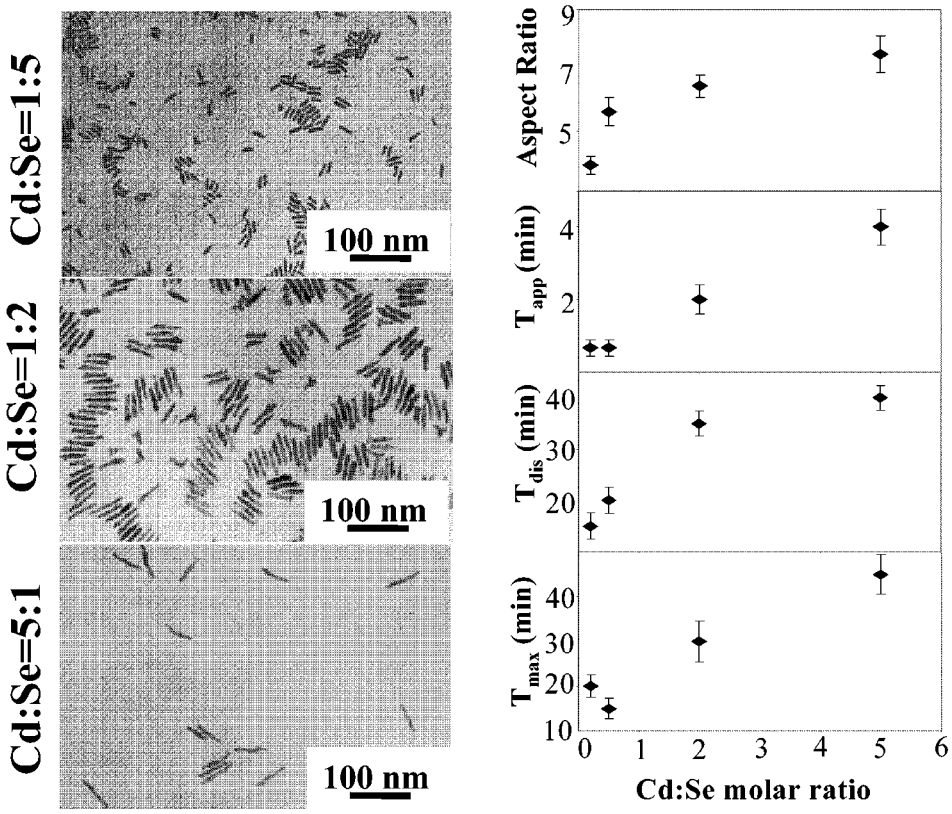

Figure 2. Left: The highest average aspect ratio of the CdSe rods in a synthesis vs the initial Cd:Se ratio of the precursors. For Cd:Se = 2:1, see the right panel picture in Figure 1. Right: The influence of the initial ratio of the Cd and Se precursors on the highest average aspect ratio of the resulting rods, the moment of the appearance of the magic sized nanoclusters (T_{app}), the moment of the disappearance of the magic sized nanoclusters (T_{dis}), and the moment for each reaction reaching the highest average aspect ratio (T_{max}).

regular nanocrystals (see Figure 1 as an example). The minimum absorption wavelength of the first exciton absorption peak of the regular nanocrystals coexisted with the magic sized nanocluster slightly shifted to red as the growth temperature increased. For the conditions shown in Figure 1 (250 °C), the minimum wavelength value of the regular nanocrystals was about 540 nm, which corresponds to CdSe nanocrystals with a diameter close to 3 nm.[25]

In the pure magic size stage, no distinguishable objects were observed under TEM, indicating the exclusive existence of the very small and TEM-invisible nanoclusters. Rod-shaped nanocrystals were found after the appearance of the absorption peak dedicated to regular sized nanocrystals, if the reaction conditions were suited for the rod growth. This result indicates that the rod's growth was initiated after the appearance of the regular nanocrystals, or these regular nanocrystals acted as the "seeds" of the anisotropically shaped nanocrystals. This explains why the minimum dimension of the short axis of the rods observed up to date was close to 3 nm.

Initial Cd to Se Precursor Ratio. The initial Cd to Se precursor ratio (Cd:Se ratio) was found as an important fact for determining the shape of the resulting nanocrystals. A series of experiments was performed with a different initial Cd:Se precursor ratio but a fixed initial concentration product of the two precursors (see Supporting Information). In Figure 2 left, each TEM image represents the aliquots with the highest average aspect ratio in a given reaction.

The general trend was that the highest average aspect ratio increased as the initial Cd:Se ratio increased as plotted in Figure 2 right, top. The moments of the appearance and disappearance of the absorption peak of the magic sized nanoclusters at 349 nm, denoted as T_{app} and T_{dis}, versus the initial Cd:Se ratio showed an almost identical trend (Figure 2 right). Moreover, the moment for a reaction to reach its highest average aspect ratio (T_{max}) was nearly identical to the values of the corresponding T_{dis}, which further demonstrates that the disappearance of the magic sized nanoclusters is indeed a quite reliable indicator of the monomer concentration in the solution as discussed above. The experimental data shown in Figure 2 indicate that the selenium precursor, Se-TBP, is more active than the cadmium precursor, Cd-TDPA. As a result, the more selenium precursor existed in the initial stage, the faster the nucleation process occurred, indicated by the T_{ap} in Figure 2 right, and the more nuclei were generated in the nucleation stage. Consequently, the remaining monomer concentration product right after the nucleation stage in the solution decreased significantly as the initial Cd:Se monomer ratio decreased, which resulted in nanocrystals with a lower aspect ratio as shown in Figure 2.

Growth with Multiple Injections. Different from the traditional multiple injections,[12] the one adopted here only replenished the selenium monomer at certain time intervals. After the primary injection, a system started with a large excess of cadmium precursor. The following secondary injections increased the total amount of selenium gradually, which eventually converted the reaction system from a cadmium excess system to a selenium excess system. The results shown in Figure 3 proved that, with multiple injections, the growth rate of the short axis was inhibited dramatically, but the aspect ratio kept increasing for the entire reaction period. Furthermore, the initial reaction conditions were identical for the two reactions shown

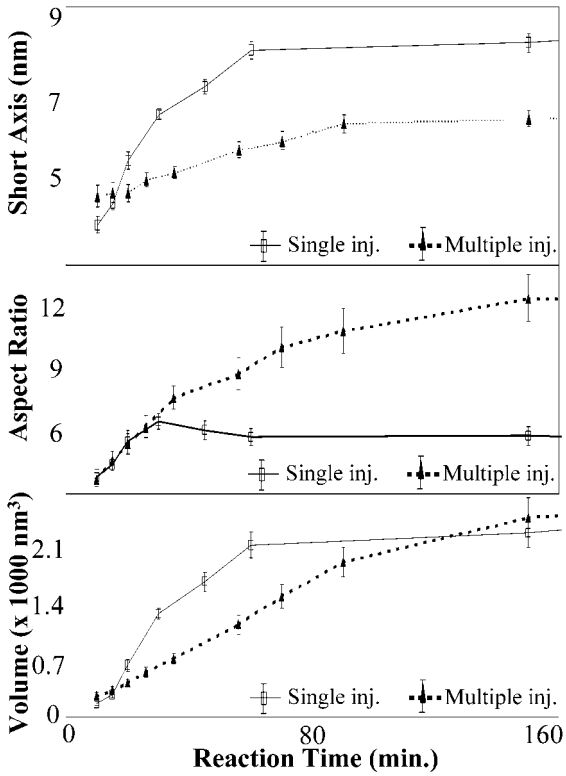

Figure 3. Influence of multiple injections on the growth kinetics of CdSe nanocrystals. The error bars represent the absolute standard deviation obtained from the statistics.

in Figure 3. Therefore, the almost overlapping positions for the points before any secondary injections took place show that the reactions in the current system are quite reproducible. This is likely because of the relatively well-controlled nucleation stage as shown in Figure 1.

Growth Direction of Rods in the 1D-Growth Stage. Potentially, there are two growth directions in the 1D-growth mode, either accumulating monomers on the (001) facet or the (00*1*) facet. The (001) and (00*1*) facets are respectively terminated with cadmium and selenium atoms for a wurtzite crystal with an equilibrium shape. Up to the present, the ligands for cationic species have been used exclusively for all growth systems for cadmium chalcogenides colloidal nanocrystals.[5,9,11,18,19] From this condition coupled with the structural nature of wurtzite structure, we proposed the growth should likely be dominated by the accumulation of monomers at the (00*1*) facet.[9] However, we did not have any experimental evidence to support this hypothesis. A similar proposal was suggested by Manna et al. after the observation of arrow-, teardrop-, and tree-shaped nanocrystals under high-resolution TEM.[11]

When the rods grew to certain lengths in the 1D-growth stage, they always turned not symmetric along the *c*-axis, with a thick but short head and a long skinny tail (Figure 4). The shape looks like a tadpole. This shape may be the so-called teardrop-shape observed by Manna et al.[11] However, Manna et al. described that the formation of the teardrop-shaped nanocrystals was a result of an Ostwald ripening process at very low monomer concentrations followed by a rapid increase of the monomer concentration by injections, instead of the straight high monomer concentrations provided in this case.

The temporal evolution of the dimensions at both ends of the tadpole-shaped nanocrystals is plotted on the bottom of Figure 4. On the skinny end, the growth rate along the *c*-axis (long axis) was about 100 times faster than that along the *a*-axis (short axis), indicating a typical 1D-growth mode.[9] On the contrast, the growth rates at the head part of the tadpoles were almost even along the short axis and the long axis of the entire structure. Importantly, the volume growth rate on both ends was about the same within the experimental and statistical errors. These results indicate that the growth at the two ends of the long axis of the entire nanocrystal is not really different in rate but in growth mode instead. At least for the relatively long rods, the growth direction is not really unidirectional. The fat end sometimes developed a multiple armed feature at the late stage of the 1D-growth, and the length of the entire structure increased significantly due to the growth along the skinny end. Because a multiarmed structure cannot be approximated to the shape drawn in Figure 4, we did not include the data in the statistics.

Growth of Close to Perfect Rods. The transformation from the rod-shape to the tadpole-shape depended on the growth temperature and the hydrocarbon chain length of the ligands (middle panel, Figure 5). In general, close to perfect rods with a high aspect ratio were generated at high temperatures and using ODPA as the ligands instead of HPA or TDPA. This is consistent with the relatively fast diffusion at high temperatures and the relatively low reactivity of the complexes with long ligands. Presumably, high temperatures should promote the diffusion flux rapidly flowing toward the fast growth facet, the (00*1*) facet, which is an ideal 1D-growth mode and yields perfect rod-shaped nanocrystals. The longer the rods are, the more difficult such directional diffusion would be, and thus the higher the temperature must be provided. The complex with long ligands may slow the diffusion rate, but its significantly low reactivity may have made a stronger impact, which provides the monomers a longer time for adjusting the position before adhering onto the surface of the nanocrystals. One example of CdSe nanocrystals with a shape close to a perfect rod grown by the mechanisms described in this paragraph is shown on the top of the middle panel in Figure 5.

The imperfection of the rod shape sometimes vanished by allowing the rods to stay in the 1D/2D-ripening stage for a certain period of time. One example is illustrated in the bottom of the middle panel of Figure 5. Another example is demonstrated in Figure 6. Evidently, in the 1D/2D-ripening stage, the driving force of minimizing the surface energy of a given nanocrystal "removed" those atoms from the relatively higher surface energy positions to the lower ones and made the nanocrystal with a relatively smooth surface.

CdSe Quantum Rice. Rice-shaped nanocrystals (left panel, Figure 5) were formed at high temperatures through the 3D-growth mode using Cd-TDPA as the precursor. The injection and growth temperatures were 350 and 300 °C, respectively. Although rice-shaped nanocrystals were observed for the reactions carried out through single injection (bottom, left panel, Figure 5), the shape of the nanocrystals was much more defined by the reactions with multiple injections (top, left panel, Figure 5), likely because of a relatively stable growth environment provided by regularly replenishing the monomer concentration.

Figure 6 illustrates the shape evolution of the rice-shaped CdSe nanocrystals through a multiple-injection reaction. The rice shape of the nanocrystals was well-developed after the reaction proceeded for about 7 min, and the system maintained

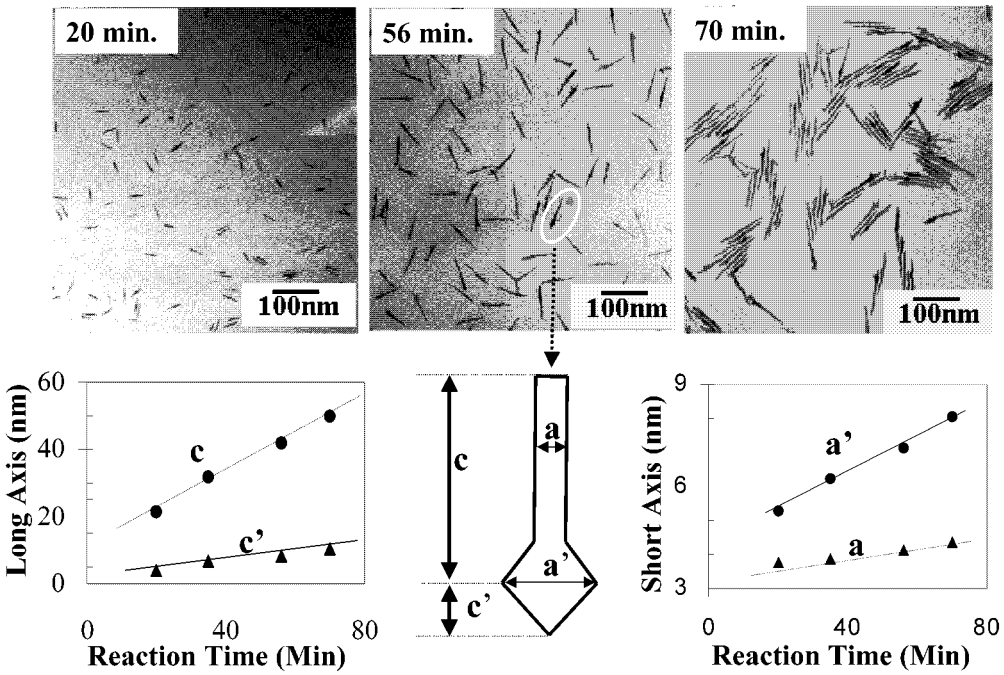

Figure 4. The shape evolution of the rod-shaped and tadpole-shaped nanocrystals.

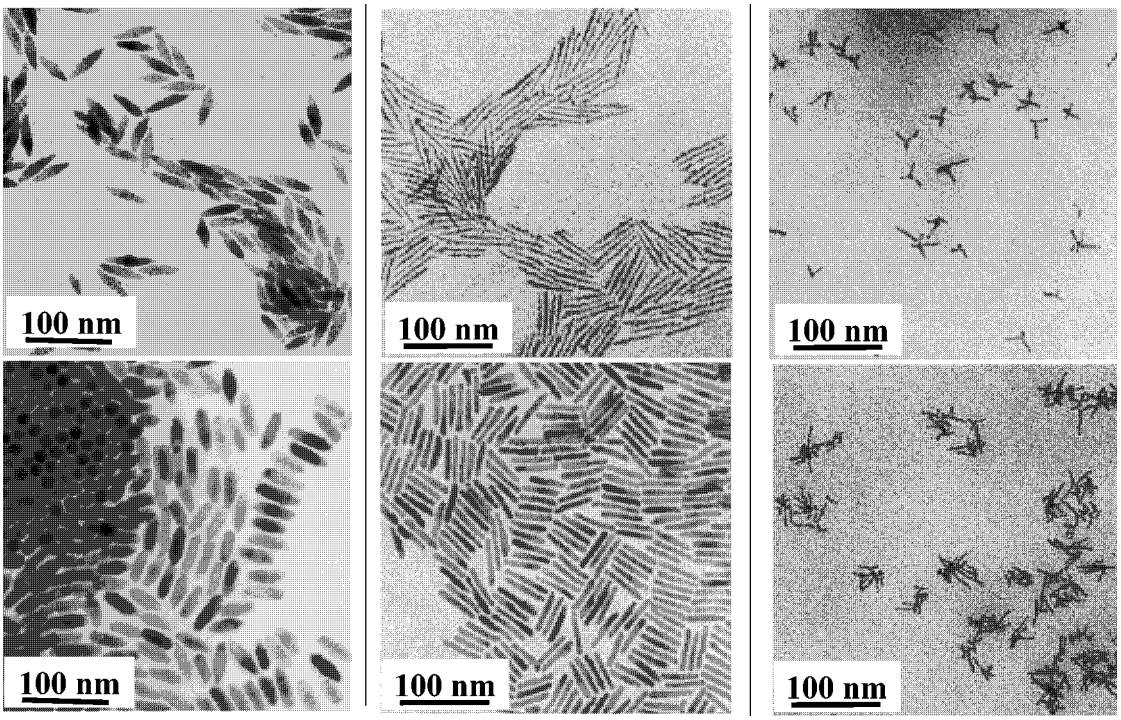

Figure 5. As-prepared CdSe nanocrystals with different shapes. Left panel: Rice-shaped nanocrystals synthesized by multiple injections (top) and by a single injection (bottom). Note: Some of the rice-shaped nanocrystals aligned with their *c*-axis perpendicular to the substrate in the bottom picture. Middle panel: Rod-shaped nanocrystals grown through straight 1D-growth mode (top) and after staying in 1D/2D-ripening for certain amount of time (bottom). Left panel: Branched nanocrystals grown at 300 °C (top) and at 180 °C (bottom).

this morphology by the injection of the selenium solution. The rice shape gradually changed to a relatively round rod shape by allowing the system to stay at the 1D/2D-ripening stage for a certain amount of time. We observed that the final products of the 1D/2D-ripening were of a dot shape.

The XRD measurements indicated that the long axis of the rice-shaped nanocrystals was also the *c*-axis of the wurtzite structure of CdSe nanocrystals. The rice-shaped nanocrystals could be useful for studying the facet-specified photochemical and chemical processes which occurred at the interface between a nanocrystal and its surroundings,[26] because these rice-shaped nanocrystals exclude any facets perpendicular to the *c*-axis.

Branched CdSe Nanocrystals. It was difficult to completely exclude the branched or multiarmed nanocrystals for the growth of rods (right panel, Figure 5). On the contrast, branched structures were not observed in the cases of the formation of

(26) Aldana, J.; Wang, Y.; Peng, X. *J. Am. Chem. Soc.* **2001**, *123*, 8844.

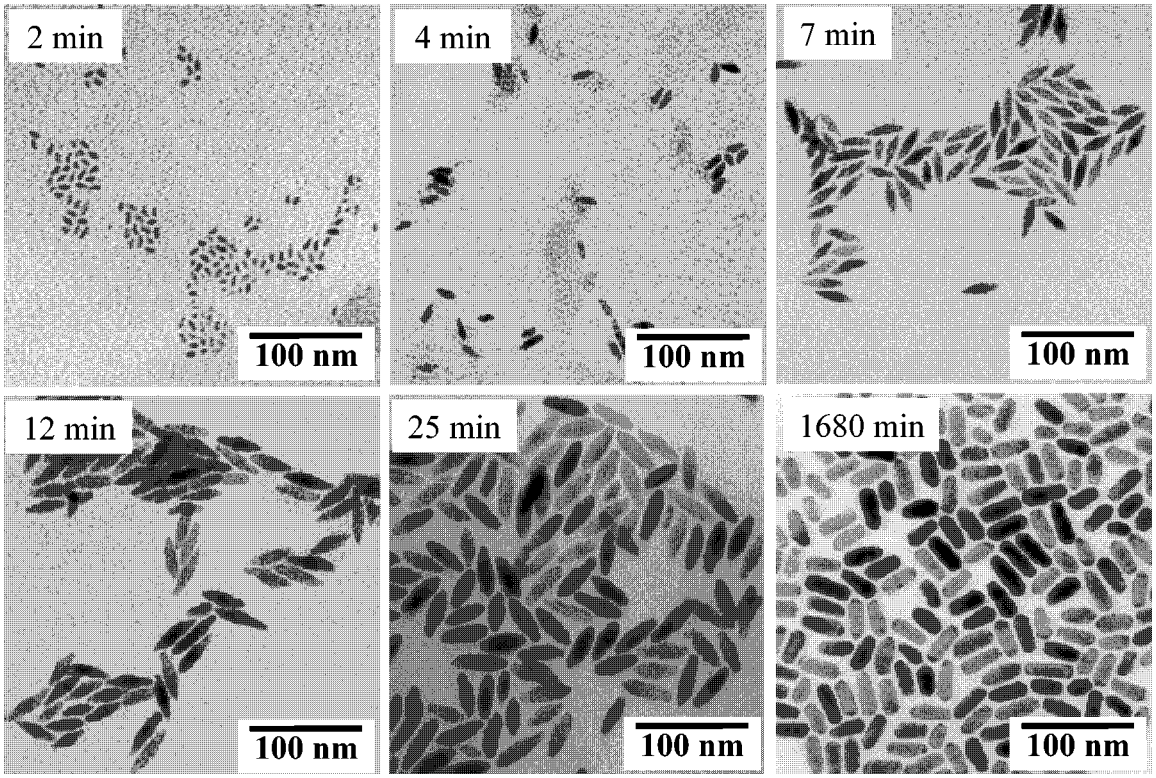

Figure 6. Temporal shape evolution of rice-shaped CdSe nanocrystals.

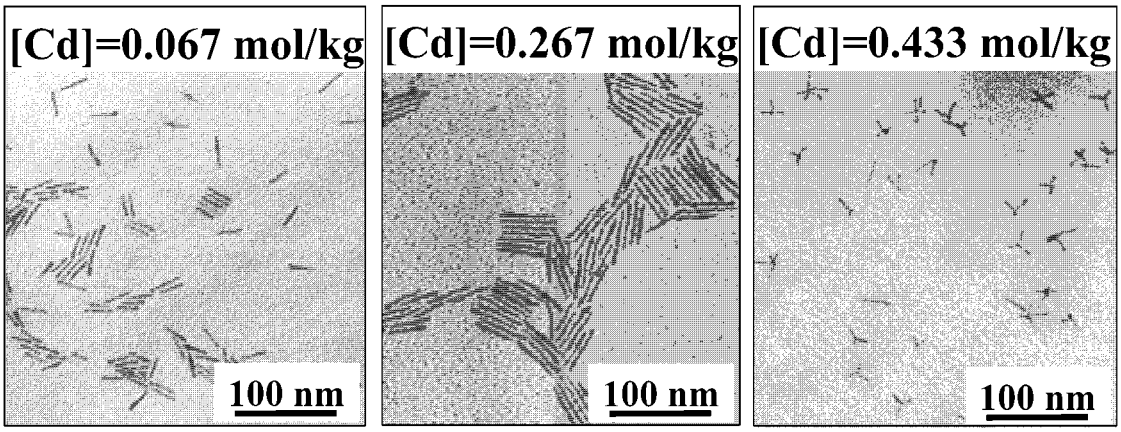

Figure 7. Monomer-concentration dependence of the shape of the resulting CdSe nanocrystals grown at 300 °C with Cd-ODPA complex as the cadmium precursor.

rice-shaped or dot-shaped nanocrystals, which occurred at relatively low monomer concentrations. At high temperatures, above 300 °C for ODPA and above 250 °C for TDPA, the population of branched nanocrystals could be limited to very few by carefully controlling the monomer concentration not higher than a certain threshold. Below these temperature limits and with very high monomer concentrations, branched nanocrystals could be dominated. In general, the lower the growth temperature was, the higher the population was, and the more branches one nanocrystal could have. This observation is qualitatively consistent with the results reported for CdS nanorods.[19]

However, the results shown in Figure 7 revealed that the formation of branched nanocrystals was directly determined by the monomer concentration in the solution. By simply increasing the precursor concentration at 300 °C, the morphology of CdSe nanocrystals varied from short rods to long rods, and then to branched ones. These results exhibit that the growth of branched nanocrystals required even higher monomer concentrations than the growth of rods in the 1D-growth mode. This requirement is not surprising from the diffusion-controlled model point of view.[9] In comparison to the single growth center at the (00*1*) facet of the rod-shaped nanocrystals, the branched ones possess multiple growth centers at the end of each branch. As a result, a relatively high diffusion flux is necessary to keep all the branches in the 1D-growth mode.

We consider that the temperature dependence of the population of the branched nanocrystals described above and reported by the others[19] is likely another form of the concentration dependence. In general, the relative supersaturation should be higher at low temperatures than that at high temperatures, if the absolute value of monomer concentration was the same. Consequently, branched nanocrystals are more favorable at low temperatures. In addition, the consumption of monomers for

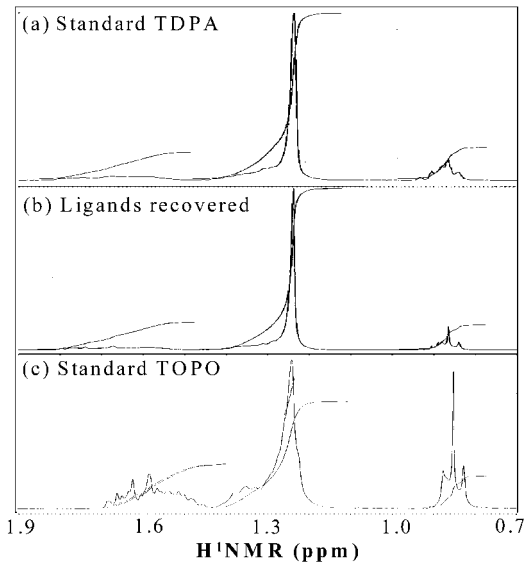

Figure 8. Ligands on the surface of CdSe rods.

the nucleation process and the number of nuclei formed at low temperatures should both be lower than those at high temperatures. This should provide a relatively high and stable monomer concentration at low temperatures, which should further benefit the formation of branched nanocrystals.

The branched nanocrystals shown in Figures 5 and 7 were readily dispersed in nonpolar solvents although they possess complicated morphology. The shape distribution of the branched nanocrystals was relatively worse than that of other shapes (see Figures 5 and 7), which is likely due to the extremely high monomer concentrations required for their growth.

Nature of the Surface Ligands. The surface capping groups of the rod-shaped nanocrystals were identified by H^1 NMR measurements. Because the signals are very broad for the ligands on the surface of nanocrystals, the experiments were performed with the free ligands isolated from the surface of nanocrystals. The experimental results shown in Figure 8 indicate that the ligands on the surface of rod-shaped nanocrystals were almost exclusively phosphonic acids (TDPA in this specific case), although there was much more TOPO than TDPA in the solution. The NMR experiments further revealed that the composition of the surface ligands for CdSe rods was independent of their aspect ratios and always dominated by phosphonic acids. These results strongly suggest that the selective surface coating by different ligands may not play a role in determining the shape of the nanocrystals.

Noncoordinating Solvent with Only TDPA as the Ligands. The growth of rod-shaped CdSe nanocrystals (Supporting Information) was observed in the newly adopted noncoordinating solvent,[27] octyldecence (ODE), using TDPA as the only ligand. This result unambiguously demonstrates that coordinating solvents and two ligands with distinguishable binding abilities are both not the prerequisites for the formation of rod-shaped nanocrystals.

Theoretical Preparation

The growth of rods in the 1D-growth mode or the 3D-growth mode requires high monomer concentrations as reported previously[5,9,11,18] and described above. Consequently, the high monomer concentrations impact the formation of nuclei. This section aims to provide a necessary theoretical basis for the further understanding of the relationship between the nucleation and the growth of shape-controlled nanocrystals.

The Gibbs−Thompson equation (eq 1) is the basis of the classic crystallization theory.[10] Although it may not be accurate enough for a quantitative description of a crystallization process in the nanometer regime, it should provide us with a starting point.

$$S_r = S_b \exp(2\sigma V_m/rRT) \tag{1}$$

where r is the radius of the crystal, σ is the specific surface energy, V_m is the molar volume of the material, S_b and S_r are the solubility of bulk crystals and crystals with a radius r, R is the gas constant, and T is the absolute temperature.

The Gibbs−Thompson equation tells us that the solubility of a given sized crystal is strongly dependent on its size. However, the solubility of a crystal with its size in nanometer regime is a relative term, since it is impossible to reach an ultimate chemical equilibrium between the nanocrystal and the monomers at the concentration S_r determined by eq 1. This is so because nanocrystals are thermodynamically mesostable species. Therefore, it should be more thermodynamically relevant to consider S_r determined by eq 1 as being a measure of the chemical potential of nanocrystals. Therefore, the chemical meaning of the Gibbs−Thompson equation is that the chemical potential of a collection of nanocrystals with a given radius r is the same as that of the monomers at the concentration S_r.

A simple mathematic treatment can change eq 1 to eq 2:

$$RT \ln S_r = RT \ln S_b + 2\sigma V_m/rRT \tag{2}$$

If μ_r and μ_b, respectively, represent the chemical potentials of the crystals with a radius r and with an infinite size, eq 2 can be converted into eq 3.

$$\mu_r = \mu_b + 2\sigma V_m/rRT \tag{3}$$

Here, we assume that crystals with different sizes share the same standard state.

For spherical crystals, the number of the surface atoms and the total atoms should be proportional to the surface area and the volume, respectively. If we define the surface atom ratio as δ, then

$$\delta = (k_1 4\pi r^2)/(k_2 4\pi r^3/3) = k_3 1/r \tag{4}$$

and k_1, k_2, and k_3 are all proportional constants.

Combining eqs 3 and 4 and setting the chemical potential of infinite sized crystals as the relative standard, the relative chemical potential of a crystal with a finite size should then be proportional to the surface atom ratio, δ.

$$\mu_r \propto \delta \tag{5}$$

Equation 5 indicates that the relative chemical potential of crystals is simply proportional to their surface atom ratio. This is understandable from a structural point of view. The difference between bulk crystals with an infinite size and crystals with a finite size is the surface atoms, which possess some dangling bonds. The average dangling bonds per atom over the entire crystal will thus determine the relative chemical potential of

(27) Yu, W. W.; Peng, X., to be submitted.

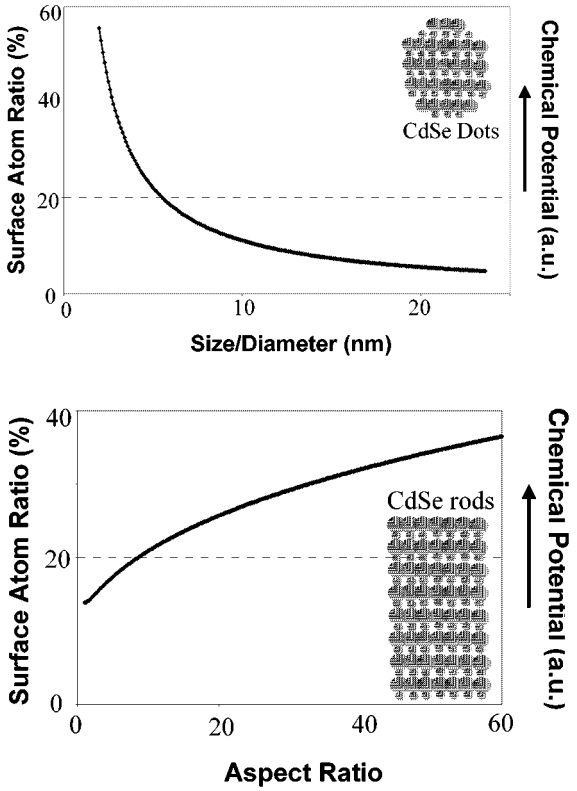

Figure 9. Top: Size-dependence of the surface atom ratio and the relative chemical potential of CdSe nanocrystals, assuming a spherical shape. Bottom: Shape-dependent chemical potential of CdSe quantum rods. The volume of all nanocrystals is set to the same value as of an 8 nm CdSe dot.

the crystal. As a result, the relative chemical potential of the crystal with a finite size should be proportional to the surface atom ratio, if we assume each surface atom of the crystal possesses the same number of dangling bonds. Notice that this assumption is actually one of the basic assumptions of the Gibbs−Thompson equation. It should be pointed out that the structural argument suggests that eq 5 should be also applicable to crystals with different shapes.

For dot-shaped crystals, their relative chemical potential is plotted in Figure 9, top, which indicates a very strong size dependence of the relative chemical potential in the nanometer regime. The shape effect on the relative chemical potential of nanocrystals with different aspect ratios is plotted in Figure 9, bottom. The volume of all the nanocrystals in Figure 9, bottom, is set to the value of an 8 nm CdSe dot. The plot reveals the strong shape dependence of the relative chemical potential of crystals. For instance, the chemical potential doubled when the CdSe crystal is elongated from an 8 nm dot to a rod with its aspect ratio equal to about 30. The related solubility change would be much more pronounced, since the factor of 2 will apply to the exponential function (eq 1).

We would like to emphasize again that, like the Gibbs−Thompson equation, the theoretical treatments in this section are based on two basic assumptions. First, all surface atoms bear the same amount of surface free energy independent of the position of the atoms, and the size or the shape of the crystals, which is equivalent to the specific surface energy argument in eq 1. Second, the relative chemical potential discussed in this section is an average value over all the atoms in a crystal. A quantitative thermodynamic consideration of crystallization in nanometer regime based on the structural

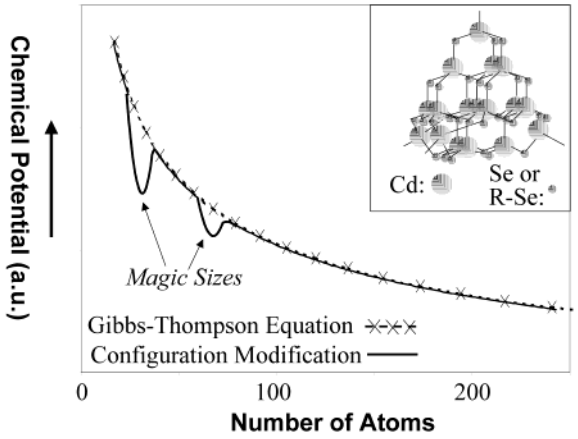

Figure 10. Schematic illustration of the size- and configuration-dependence of the relative chemical potential of crystals/clusters in the extremely small size regime. Inset: Structure of Cd17.[25] The magic sized nanocluster observed in this work may likely possess a similar structure.

argument described above is in development, which aims to remove these two assumptions.

Discussion

When a crystallization system starts by quickly mixing two precursors together, the classical nucleation theory determines the minimum stable size of the nuclei to be formed in the solution using the Gibbs−Thompson equation (eq 1).[10] These smallest stable nuclei are called critical nuclei, whose solubility determined by the Gibbs−Thopson equation is equal to the monomer concentration (or monomer concentration product depends on the definition) in the solution. Anything smaller than these critical nuclei will be dissolved promptly. Any clusters/crystals larger than the critical nuclei should have a lower chemical potential than the monomers in the solution, and thus should grow to even larger sizes. In principle, the higher the monomer concentration is, the smaller the critical nuclei can be, and the easier the nucleation process can take place.

The intrinsically high relative chemical potential of the rods on average (Figure 9, bottom) requires the system to maintain a high monomer concentration. This equilibrium concentration is close to the one at the 1D/2D-ripening stage. If the growth is in 1D-growth mode,[9] the monomer concentration should be even significantly higher. In principle, the 1D-growth occurs only if the chemical potential of the monomers in the solution is much higher than the highest chemical potential of the atoms on the surface of nanocrystals, which are those on the two unique facets perpendicular to the *c*-axis for wurtzite CdSe nanocrystals.[9]

Such a high monomer concentration complicates the nucleation process as described in the Results section. The critical nuclei can be much smaller than the ones observed for the synthesis of dots. In this extremely small size range, the relative chemical potential is extremely size dependent and very sensitive to the configuration of the nuclei. This is why we always observed the formation of magic sized nanoclusters, which are those clusters with local minimum chemical potential because of their close-shell configurations. Certainly, the Gibbs−Thompson equation is no longer valid in this size regime. Schematically, Figure 10 illustrates the size and configuration dependence of the relative chemical potential in this extremely small size regime.

The inevitable formation of magic sized nanoclusters in the nucleation stage for the growth of anisotropic shapes likely plays

a key role in determining the nature of all of the following events, and the size/shape of the resulting nanocrystals. The magic sized nanoclusters promote the formation of rods or other anisotropic structures always with a nearly monodisperse lateral dimension regardless of the distribution of the aspect ratio. If the system is limited to the formation of one kind of magic sized nanoclusters as in the current system, the initiation of the rod's growth always starts from the instant when some magic sized nanoclusters "tunnel" through the lower thermodynamic barrier on the side toward larger sizes (see Figure 10), denoted as forward-tunneling. The lateral dimension of the rods in the 1D-growth mode is thus set as a more or less fixed value.

The fate of those magic sized nanoclusters may have several pathways, in addition to the forward-tunneling to grow bigger almost instantaneously and grow longer in the following 1D-growth or 3D-growth stage. It may decompose to monomers by "tunneling" through the high barrier on the reverse direction, denoted as backward-tunneling. Obviously, a relatively low monomer concentration will benefit the backward-tunneling in two ways. First, the forward-tunneling requires the addition of a fairly large amount of monomers onto the magic sized nanoclusters to convert them into the regular nanocrystals with much larger sizes (see UV−vis spectra shown in Figure 1). The addition of a large amount of monomers to the magic sized clusters should occur in a very rapid way if it is not instantaneous, because no intermediate sized clusters/crystals between the magic sized clusters and the resulting regular sized nanocrystals of the forward-tunneling process were observed by UV−vis measurements (Figure 1). A relatively high monomer concentration will greatly enhance such an event. Second, the final products of the backward-tunneling event are monomers, whose chemical potential is associated with the monomer concentration in the solution. The lower the monomer concentration in the solution is, the more stable the products of the backward-tunneling can be.

Because the quantum rices were grown in the 3D-growth regime, the relative chemical potential of the remaining monomers in the growth stage was relatively low. Consequently, the backward-tunneling should be dominated shortly after the initial growth of the rice-shaped nanocrystals. Therefore, the distributions of both lateral dimension and the aspect ratio were nearly monodisperse, and the formation of the branched nanocrystals was prohibited (see discussions below). Overall, if the distribution of the aspect ratio of the resulting rods, rices, and other related nanostructures was narrow, a fair amount of the magic sized nuclei should have gone through the backward-tunneling shortly after the nucleation stage.

The magic sized nuclei can also explain the formation of multiarmed or branched structures formed at very high monomer concentrations. A handful of magic sized nanoclusters of cadmium chalcogenides with identified molecular (crystal) structures have been reported.[25,28−30] All of those are with a tetrahedron close-shell configuration and a zinc blend bonding geometry of the core, no matter what the growth temperature was. We tentatively think this is a result of the suitability to form a close-shell structure of the zinc blend structure.

The absorption peak position (349 nm) of the magic sized nanoclusters observed in the current system resembles that of the Cd17 cluster shown in Figure 10, inset. On the basis of this experimental observation and the unique zinc blend core feature of all of the CdSe and CdS magic sized clusters reported so far,[25,28−30] we tentatively suggest that the magic sized nanoclusters formed in the current system also have a tetrahedron close-shell configuration with a zinc blend core. This assumption is highly consistent with the formation of the observed branched nanostructures. High-resolution TEM studies revealed that the branching point of these complicated structures is always a tetrahedron core with zinc blend structure, although the rest of the nanocrystals are in wurtzite structure.[11,19] Likely, the structure and morphology of the magic sized nanoclusters are arrested in those branching points. Furthermore, the experimental results described above and reported by others revealed that the branched structures are more likely to appear at lower growth temperatures.[19] This is also consistent with the stability of the zinc blend structures at lower temperatures. Presumably, a phase transition to wurtzite structure may easily take place at higher temperatures when the magic sized nanoclusters go through a forward-tunneling to become the real seeds for the growth of the elongated structures.

Conclusion

The nucleation process of colloidal semiconductor nanocrystals was assessed for the first time. The growth mechanisms of colloidal CdSe quantum rods and other anisotropic structures are complicated by the required high monomer concentrations, which dramatically impact the initial nucleation stage. A unique magic sized nanocluster with the first absorption peak at 349 nm was found as the common nuclei for the growth of CdSe quantum rices, tadpoles, rods, and branched-nanocrystals. This means that the classic nucleation model, the Gibbs−Thompson equation, is no longer valid for predicting the size of the critical nuclei. A new model, which takes this configuration dependence of the relative chemical potential of crystals (clusters), is needed. The magic sized nuclei deeply impact the following growth processes of the elongated nanostructures. Experimental results indicate that the formation of magic sized nuclei must be taken into account for designing a successful synthetic scheme for any given type of anisotropic CdSe nanostructures. With the knowledge described in this paper, nearly monodisperse CdSe nanocrystals with a variety of elongated shapes have been reproducibly synthesized with an exceptional control over their sizes along all three dimensions. Furthermore, the development of the shape-controlled synthesis of semiconductor nanocrystals was found compatible with the implementation of green chemical principles into the related synthetic chemistry. Specifically, relatively stable alternative cadmium precursors were found advantageous for developing the shape-controlled synthesis for CdSe nanocrystals in comparison to the traditional organometallic precursor, $Cd(CH_3)_2$.

Acknowledgment. This work is financially supported by the NSF Career Award (DMR-0094248), the NSF CHE-0101178 grant.

Supporting Information Available: Experimental details and a TEM image of CdSe rods formed in the noncoordinating solvent (PDF). This material is available free of charge via the Internet at http://pubs.acs.org.

JA0173167

(28) Vossmeyer, T.; Reck, G.; Schulz, B.; Haupt, E. T. K.; Weller, H. *Science* **1995**, *267*, 1477.
(29) Herron, N.; Calabress, J. C.; Farneth, W. E.; Wang, Y. *Science* **1993**, *259*, 1426.
(30) Dance, I. G.; Choy, A.; Scudder, L. *J. Am. Chem. Soc.* **1984**, *106*, 6285.